



Contents lists available at ScienceDirect

## Quaternary Science Reviews

journal homepage: [www.elsevier.com/locate/quascirev](http://www.elsevier.com/locate/quascirev)

Invited review

## Chronostratigraphy of the 600,000 year old continental record of Lake Van (Turkey)

Mona Stockhecke<sup>a,b,\*</sup>, Ola Kwiecien<sup>a,b,c</sup>, Luigi Vigliotti<sup>d</sup>, Flavio S. Anselmetti<sup>e</sup>, Jürg Beer<sup>a</sup>, M. Namik Çağatay<sup>f</sup>, James E.T. Channell<sup>g</sup>, Rolf Kipfer<sup>h,i,j</sup>, Johannes Lachner<sup>a</sup>, Thomas Litt<sup>k</sup>, Nadine Pickarski<sup>h</sup>, Michael Sturm<sup>a</sup>

<sup>a</sup> Eawag, Swiss Federal Institute of Aquatic Science and Technology, Department of Surface Waters Research and Management, Ueberlandstrasse 133, P.O. Box 611, 8600 Dübendorf, Switzerland

<sup>b</sup> ETH, Geological Institute, Zurich Universitaetsstrasse 5, 8092 Zurich, Switzerland

<sup>c</sup> Ruhr-University Bochum, Universitaetstrasse 150, 44801 Bochum, Germany

<sup>d</sup> Istituto di Scienze Marine, ISMAR-CNR, Bologna, Italy

<sup>e</sup> Institute of Geological Sciences and Oeschger Centre for Climate Change Research, University of Bern, Baltzerstrasse 1-3, 3012 Bern, Switzerland

<sup>f</sup> Department of Geological Engineering and Eastern Mediterranean Centre for Oceanography and Limnology, Istanbul Technical University, Maslak, 34469 Istanbul, Turkey

<sup>g</sup> Department of Geological Sciences, University of Florida, Gainesville, FL 32611, USA

<sup>h</sup> Swiss Federal Institute of Aquatic Science and Technology, Water Resources and Drinking Water, Eawag, Ueberlandstrasse 133, P. O. Box 611, 8600 Dübendorf, Switzerland

<sup>i</sup> Institute of Biogeochemistry and Pollutant Dynamics, Swiss Federal Institute of Technology (ETH), Universitaetstrasse 16, 8092 Zurich, Switzerland

<sup>j</sup> Institute of Geochemistry and Petrology, Swiss Federal Institute of Technology (ETH), Clausiusstrasse 25, 8092 Zurich, Switzerland

<sup>k</sup> Steinmann Institute of Geology, Mineralogy and Paleontology, Bonn University, Nussallee 8, 53115 Bonn, Germany

## ARTICLE INFO

## Article history:

Received 8 August 2013

Received in revised form

25 March 2014

Accepted 8 April 2014

Available online xxxx

## Keywords:

ICDP project PALEOVAN

Long terrestrial paleoenvironmental records

Climatostratigraphic alignment

Radiometric dating

Tephrostratigraphy

Magnetostratigraphy

## ABSTRACT

Lake Van sediment cores from the Ahlat Ridge and Northern Basin drill sites of the ICDP project PALEOVAN contain a wealth of information about past environmental processes. The sedimentary sequence was dated using climatostratigraphic alignment, varve chronology, tephrostratigraphy, argon–argon single-crystal dating, radiocarbon dating, magnetostratigraphy, and cosmogenic nuclides. Based on the lithostratigraphic framework, the different age constraints are compiled and a robust and precise chronology of the 600,000 year-old Lake Van record is constructed. Proxy records of total organic carbon content and sediment color, together with the calcium/potassium-ratios and arboreal pollen percentages of the 166-m-long event-corrected Ahlat Ridge record, mimic the Greenland isotope stratotype (NGRIP). Therefore, the proxy records are systematically aligned to the onsets of interstadials reflected in the NGRIP and synthesized Greenland ice-core stratigraphy. The chronology is constructed using 49 age control points derived from visual synchronization with the Greenland ice-core stratigraphy using the GICC05 timescale, an absolutely-dated speleothem timescale (e.g., Hulu, Sanbao, Linzhu cave) and the Epica Dome C timescale. In addition, the uppermost part of the sequence is complemented with four ages from Holocene varve chronology and three calibrated radiocarbon ages. Furthermore, nine argon–argon ages and a comparison of the relative paleointensity record of the magnetic field with reference curve PISO-1500 confirm the accuracy of the age model. Also the identification of the Laschamp event via measurements of  $^{10}\text{Be}$  in the sediment confirms the presented age model. The chronology of the Ahlat Ridge record is transferred to the 79-m-long event-corrected composite record from the Northern Basin and supplemented by additional radiocarbon dating on organic macro-remains. The basal age of the Northern Basin record is estimated at ~90 ka. The variations of the time series of total organic carbon content, the Ca/K ratio, and the arboreal pollen percentages illustrate that the presented chronology links ice-marine-terrestrial stratigraphies and that the paleoclimate data are suited for reconstructions and modeling of the Quaternary and Pleistocene climate evolution in the Near East at millennial timescales. Furthermore, the chronology of the last 250 ka can be used to test other dating techniques.

© 2014 Elsevier Ltd. All rights reserved.

\* Corresponding author. Eawag, Swiss Federal Institute of Aquatic Science and Technology, Department of Surface Waters Research and Management, Ueberlandstrasse 133, P.O. Box 611, 8600 Dübendorf, Switzerland. Tel.: +41 58 765 5508; fax: +41 58 765 5210.

E-mail address: [mona.stockhecke@eawag.ch](mailto:mona.stockhecke@eawag.ch) (M. Stockhecke).

## 1. Introduction

Lake sediments constitute valuable terrestrial archives of past environmental conditions. They are potentially continuous over several Interglacial/Glacial cycles and, ideally, varved, providing annually-resolved to seasonally-resolved records at sub-millennial timescales. An excellent example is the sedimentary sequence recovered from two sites in Lake Van (Turkey) by the PALEOVAN project of the International Continental Drilling Program (ICDP). The two drill sites, Northern Basin (NB) and Ahlat Ridge (AR) are located in the north western part of Lake Van at water depths of 245 m and 360 m (relative to present lake level at ~1650 m above sea level), respectively. AR – the primary site – is a morphological ridge at the northern edge of the 440 m-deep Tatvan Basin. This special volume presents several multidisciplinary contributions of the PALEOVAN scientific team. The rationale for this study is to deliver and discuss a common chronology for paleoenvironmental investigations. General information about the pre-site survey are given in Litt et al. 2009 and about the project, the drilling operations and sampling party are given in Litt et al. (2012).

A robust age model is mandatory for a comprehensive temporal understanding of the environmental information in sedimentary archives. Terrestrial archives, and in particular the sediment of Lake Van, are also influenced by non-climate driven changes. Tectonic and volcanic activity causes post-depositional deformation, and resultes in mass-movement deposits and volcanoclastic layers (Stockhecke et al., 2014). Two major gaps occur in the composite AR record (at ~125 and ~170 m bblf, meters composite depth below lake floor) and the lowermost part of the NB record shows several unconformities. The lithostratigraphic framework (Stockhecke et al., 2014) takes all these processes into account in order to extract an event-corrected succession reflecting solely background sedimentation, and thus providing the backbone for the age model. Another characteristic lithological feature is the frequent intercalation of event deposits coinciding with each glacial termination and with the well expressed interstadials (Stockhecke et al., 2014).

The stratigraphic correlation between the PALEOVAN drill sites is used for extrapolating the AMS-<sup>14</sup>C ages of terrestrial macro-remains from the NB record to the AR record. This enables the transfer of the AR chronology to the NB record. The stratigraphic correlation with previously recovered sediment cores (Landmann et al., 1996; Lemcke, 1996; Lemcke and Sturm, 1997) offers the advantage of transposing a varve chronology for the Holocene.

The lithostratigraphic framework of both drill sites documents that: i) lake-level variations expressed by abruptly changing lithologies and total organic carbon content were controlled by global climate changes, ii) climate-sensitive proxy records can be aligned with Greenland Stadials (GS) and Interstadials (GIS) and Marine Isotope Stages (MIS) and iii) volcanic events and associated tephras frequently intercalating the background sediments are datable (<sup>40</sup>Ar/<sup>39</sup>Ar single-crystal dating) at least back to ~530 ka (Stockhecke et al., 2014). Consequently, the terrestrial archive of Lake Van provides a unique opportunity to apply both absolute and relative dating methods to records from both drill sites. To align ice-core and terrestrial records, several proxies reflecting independent processes, such as lake productivity and catchment processes, are used in combination to enhance the fidelity of the correlations.

The marine isotope stack LR04 (Lisiecki and Raymo, 2005) covering several millions of years, provides a recognized reference for correlating marine and terrestrial records at Glacial/Interglacial timescales (Melles et al., 2012), but is of inappropriate resolution for centennial/millennial-scale comparison. The

overall good agreement of Glacial/Interglacial and stadial/interstadial variability expressed in the Lake Van sedimentary proxies invites comparison with other high-resolution archives. Millennial-scale reference templates include: i) the uppermost 60 ka of the NGRIP ice cores on the GICC05 timescale (NGRIP, 2004; Steffensen et al., 2008; Svensson et al., 2008; Wolff et al., 2010) and ii) the 400 kyr-old Chinese speleothem records (Wang et al., 2008; Cheng et al., 2009). Moreover, Barker et al. (2011) constructed a 800 kyr-old synthetic record of Greenland climate variability based on the thermal bipolar seesaw model (Broecker et al., 1990). They showed that millennial-timescale variability occurred in Greenland throughout the last 800 kyr and, by tying their model to the Chinese speleothem chronology, they provide a refined absolute age scale back to ~400 ka. By choosing absolutely dated speleothems, Barker et al. (2011) set their model free from dependence on orbital cycles underlying the Epica Dome C timescales (EDC; Jouzel et al., 2007). The expressions of interstadials/stadials in the Lake Van record, combined with a reference record resolving millennial-scale variability, provide the opportunity to use chronostratigraphic alignment to date the complete ~600 kyr-old record of Lake Van. Additionally, the comprehensive catalog of dated volcanic events in eastern Anatolia back to 400 ka (~40 recognized fallout and pyroclastic flows; Sumita and Schmincke, 2013a,b,c) hold the promise of the Lake Van record becoming one of the most precise tephrostratigraphic chronologies, cross-validated using geochemical fingerprinting.

Another method to date the Lake Van sediment is based on the paleomagnetic record of relative paleointensity (RPI) variations (Vigliotti et al., this issue). Matching these data with reference templates (i.e. stacked PISO-1500 record; Channell et al., 2009) provides robust stratigraphic tie-points, especially considering that the RPI is a global geophysical (geomagnetic) signal devoid of environmental influences. A prominent RPI minimum associated with the Laschamp geomagnetic excursion, accompanied by natural remanent magnetization (NRM) directions with negative inclinations representing the directional expression of the excursion, provides an especially useful chronostratigraphic marker. The Laschamp geomagnetic excursion is well-dated radiometrically (41.3 ± 0.6 ka BP, Laj et al., 2014; 40.70 ± 0.95 ka BP, Singer et al., 2009), by astrochronology (~41 ka BP, Laj and Channell, 2007) and consistent with the pronounced peak in <sup>10</sup>Be flux associated with the Laschamp event found in the NGRIP (GICC05 age of Laschamp magnetic event: 41.2 ± 1.6 ka BP, Svensson et al., 2008). It demarcates the center of Daansgaard–Oeschger event 10 (GIS-10) in Greenland isotope record (NGRIP), which is also identified in terrestrial counterparts (e.g. Hulu Cave in China, Wang et al., 2001), so that the identification of the Laschamp event provides a relative time marker, which links to ice-core stratigraphies (from Greenland and Antarctica), speleothem and paleomagnetostratigraphic records (e.g., Austin and Hibbert, 2010).

To sum up, this contribution compiles a range of relative and absolute age constraints produced by several independent methods in order to overcome the limitations and shortcomings of each single method and to establish one common chronology for the ~600 kyr-old Lake Van record. A robust and precise age model is an essential prerequisite for understanding the climate response to external forcing, for comparison of different records and data synthesis, and for resolving the successions and consequences of climate changes. Moreover, its outcome might help to improve calibration standards for other dating techniques (e.g., AMS-<sup>14</sup>C, <sup>40</sup>Ar/<sup>39</sup>Ar, Uranium–Thorium dating of autochthonous carbonate, optical stimulated luminescence and thermoluminescence).

## 2. Dating methods

### 2.1. Event-corrected composite records and stratigraphic correlation

The lithostratigraphy of the Lake Van records distinguishes three main sediment groups: i) lacustrine clayey silt, ii) volcanoclastics and iii) coarse grained fluvial deposits. The lacustrine clayey silt group consists of eight lithologies, each reflecting different lake states along with one group (graded beds, Lg) reflecting regional events (Stockhecke et al., 2014). The event-corrected composite records of 166 m from AR, and 79 m from NB, represent only the lacustrine clayey silt without the event layers. The event-corrected records of both sites are used to construct the age model. Marker layers from the correlation of the two drill sites (Stockhecke et al., 2014) are taken to transpose ages between the drill sites.

### 2.2. Proxy data

Proxy records of total organic carbon content (TOC; details in Stockhecke et al., 2014, Fig. 1) also reflected in the sediment color

(reflectance b\*), calcium and potassium elemental ratios (Ca/K) measured by X-ray fluorescence (XRF; details in Kwiecien et al., this issue) and arboreal pollen (details in Litt et al., this issue), were used for age model construction. The TOC samples were taken at 2.5-cm increments over most of the AR composite record and at 20-cm increments over the NB composite record. Continuous 0.3-mm-resolved color reflectance data were exported from high-resolution core photographs taken with a Color Line Scan camera. XRF Core Scanner data were collected every 2 cm downcore over the whole composite profile of the AR. Arboreal pollen percentages (AP; ratio between tree and herbs) from paleontological analysis were carried out on discrete samples collected at the same levels as those used for geochemical analysis at 20-cm increments from 0 to 60 mcbf of the AR composite record and at 1-m increments for 60–220 mcbf.

### 2.3. Reference timescales to align climate-sensitive proxy records

The proxy records were visually aligned to the GICC05/GICC05modeltext-based NGRIP isotopic record (0–116 ka BP; NGRIP, 2004; Steffensen et al., 2008; Svensson et al., 2008; Wolff et al., 2010) and the speleothem-based (116–400 ka BP) and

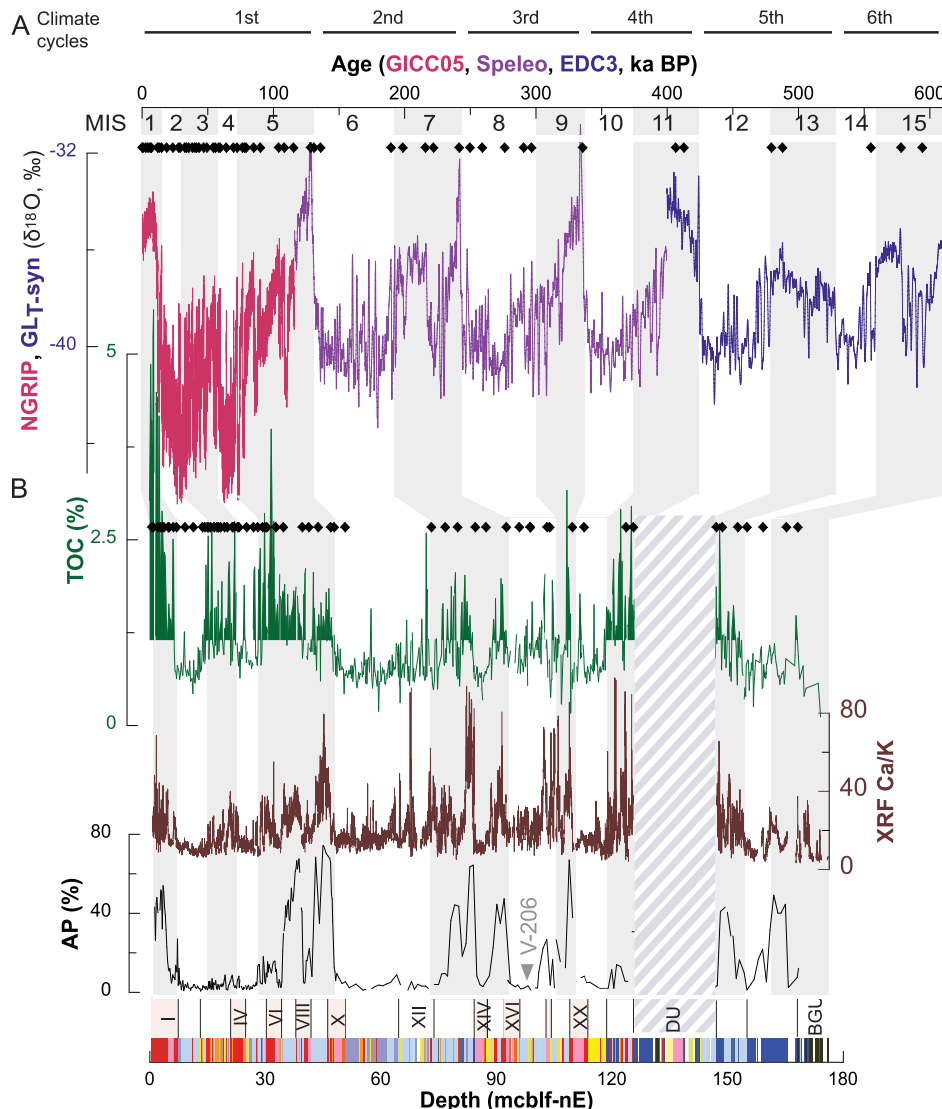


**Fig. 1.** Comparison of Greenland stratigraphy and paleoclimate proxy records from the AR. Diamonds indicate proposed age control points between the reference record and the proxy data. A. The NGRIP/GLT-syn  $\delta^{18}\text{O}$  ( $\text{\textperthousand}$  VSMOW) records from Greenland over the last 600 kyr. B. Event-corrected AR composite records of total organic carbon (TOC) contents, XRF Ca/K ratio, arboreal pollen (AP), lithological units and the lithostratigraphy (key in Fig. 4) over the 175 mcbf-nE.

EDC3-based (400–650 ka BP) synthetic Greenland record (GLT-syn; Barker et al., 2011, Fig. 1). Instead of using one continuous but orbital-dependent EDC-timescale of lower resolution over the ~600 ka, we integrated three reference records, each with a resolution matching that of the Lake Van profile in the respective interval. This procedure involves two discontinuities at 116 ka and at 400 ka in order to link to the Lake Van record to the highest-resolved and absolutely-dated time reference templates. The absolute ages facilitate comparison with, for instance, discontinuous speleothem records from other regional archives such as Sofular cave (Fleitmann et al., 2009) or Soreq cave (Bar-Matthews et al., 1999).

#### 2.4. Alignment of proxy data

The climate-sensitivity of the proxy records is reflected in their resemblance to Greenland temperature variability (Fig. 1). The NGRIP  $\delta^{18}\text{O}$  stratotype is apparently replicated in records from Lake Van. The temperature variations over Greenland are probably transmitted to Lake Van by atmospheric circulation changes controlling precipitation and the net water budget. High lake levels

are apparent in warm interstadials/interglacials and low lake levels for the cold stadials/glacials (Stockhecke et al., 2014). This pattern is reflected in TOC-rich brown laminated (TOC-poor gray bioturbated or banded) sediment (Stockhecke et al., 2014) containing high (low) Ca/K intensities (Stockhecke et al., 2014; Kwiecien et al., this issue; Çağatay et al., this issue). Because the interstadial onsets are reported as a consistent universal pattern (Wang et al., 2008; Cheng et al., 2009; Deplazes et al., 2013) and can be clearly identified as increases in TOC/b\* and Ca/K, only the onsets were aligned to the interstadial onsets of the NGRIP  $\delta^{18}\text{O}$  record. The number of events identified is comparable to the peaks of the lower-resolution AP record, supporting synchronicity between internal lake responses and the vegetation dynamics and providing a mechanistic link for decreased input of detrital material (Ca/K) during warmer intervals when vegetation was thriving. Lead/lags between the proxy records are difficult to assess due to their differing resolutions, but the AP increase generally seems to lag behind the TOC increase. The minimal tuning approach incorporates the assumption of regular sediment accumulation rates between the age control points. For the intervals showing increased frequency of event deposits

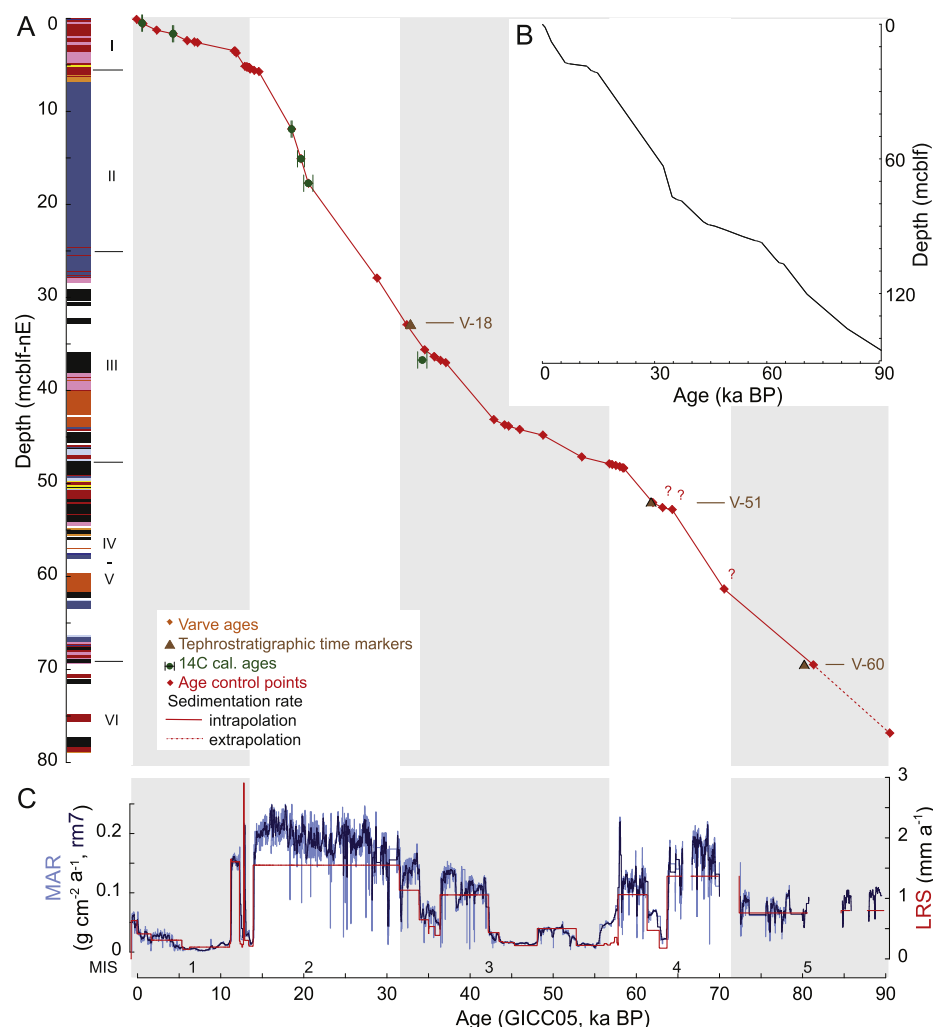


**Fig. 2.** Chronostratigraphic framework of the Lake Van NB record over the last 90 ka BP. A. Lithostratigraphy (key in Fig. 4) and age/depth model for Lake Van NB event corrected composite record (mcblf-nE) with the tie points of AMS- $^{14}\text{C}$  calibrated ages, tephrostratigraphic ages (Sumita and Schmincke, 2013c), and age control points derived from the correlation of the AR record. Linearly regressed age control points are illustrated in red. B. Age/depth model for NB composite record (mcblf). C. Mass-accumulation rates (MAR) and linear sedimentation rates (LSR) of the NB record.

**Table 1**

Depth and ages of the seven RPI minima (a–g) and the interval of increased  $^{10}\text{Be}$  fluxes (Laschamp) associated to the Laschamp event identified in the AR record in comparison with the ages from literature. The paleomagnetic record shows reverse polarity in correspondence to Laschamp only over few centimeters here defined as aL. The overall error estimate of the ages of the RPI minima is about  $\sim 1$  ka.

Depth (mcbf)		Depth (mcbf-nE)		Age (ka BP)		Label	Age (ka BP)		Reference
Top	Bottom	Top	Bottom	From	To		From	To	
20.06	21.60	16.28	17.64	38.8	43.0	a	41.3 ± 0.6		Laj et al., 2014
20.09	20.16	16.31	16.38	38.8	39.0	aL	41.3 ± 0.6		Laj et al., 2014
29.94	30.19	24.32	24.53	63.9	64.6	b	63	64	Channell et al., 2009
46.41	48.22	36.72	38.46	96.6	103.1	c	97	101	Channell et al., 2009
52.89	55.36	42.35	44.49	114.7	122.6	d	119	122	Channell et al., 2009
103.46	104.45	82.07	82.98	214.1	216.7	e	210	213	Channell et al., 2009
111.81	112.58	89.07	89.82	237.3	240.1	f	238	240	Channell et al., 2009
119.51	120.33	94.82	95.64	256.9	259.4	g	256	258	Channell et al., 2009
19.8	20.7	16.02	16.87	38.1	40.3	Laschamp	41.3 ± 0.6		Laj et al., 2014

(terminations and pronounced interstadials), additional tie points were set. The resultant 62 age control points constitute: 56 'real' tuning points, two tie points set to mark the sediment–water interface, and lacustrine sediment–fluvial deposits at the base, and four tie points to set the gaps by extrapolation.

## 2.5. Varve counting

Four marker layers allow for reliable use of four varve ages for dating of the uppermost meters of the PALEOVAN records (varve chronology by Landmann et al., 1996; Lemcke, 1996, 1997).

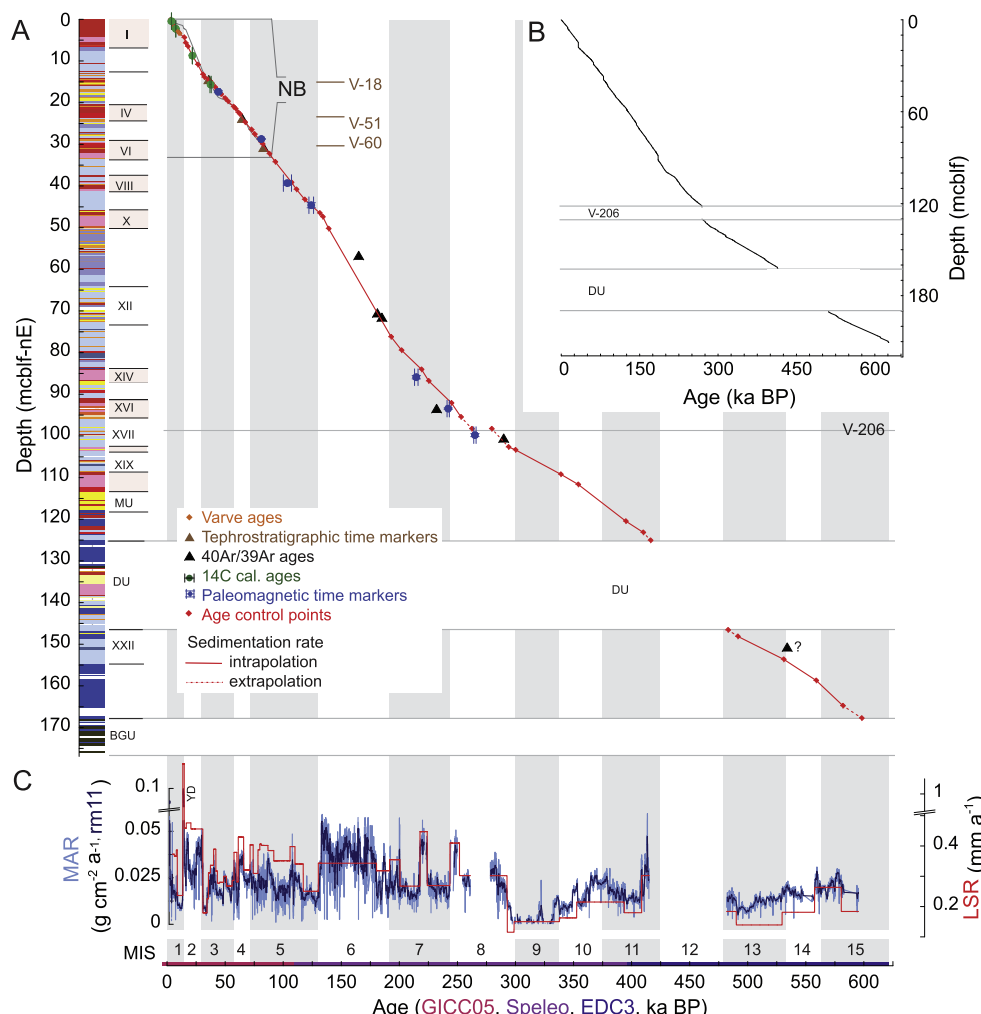


**Fig. 3.** Chronostratigraphic framework of the AR record over the last  $\sim 600$  kyr. A. Lithostratigraphy (key in Fig. 4) and age/depth model for Lake Van AR event corrected composite record (mcbf-nE) with the tie points of AMS- $^{14}\text{C}$  calibrated ages, tephrostratigraphic ages (Sumita and Schmincke, 2013c),  $^{40}\text{Ar}/^{39}\text{Ar}$  ages (Stockhecke et al., 2014) and age control points derived from the correlation of Lake Van paleoclimate records to ice core  $\delta^{18}\text{O}$  record of NGRIP/GLT-syn (see text for references) and Lake Van paleomagnetic PISO-1500 stack (Channell et al., 2009). The bars of the paleomagnetic points represent duration of each event as given in Table 1. Linearly regressed tie points are in red. B. Age/depth model for Lake AR composite record (mcbf). C. Mass-accumulation rates (MAR) and linear sedimentation rates (LSR) of the AR record.

## 2.6. Tephrostratigraphy

Three volcaniclastic layers (V-18, V-51 and V-60; Stockhecke et al., 2014) correspond to the onshore dated ~30 ka Nemrut Formation (NF), ~60 ka Halepkalesi Pumice-10 (HP-1) and ~80 ka Incekaya-Dibeli Tephra (Sumita and Schmincke, 2013a).

## 2.7. $^{40}\text{Ar}/^{39}\text{Ar}$ ages

Reliable ages of six  $^{40}\text{Ar}/^{39}\text{Ar}$  single crystal dated tephra layer from ~162 ka BP to ~531 ka BP are available for cross-evaluation (Stockhecke et al., 2014).

## 2.8. $\text{C}14$ ages

Six calibrated AMS radiocarbon ages from 0.6 to 34 ka BP derived from terrestrial macro-remains from turbidite deposits from the NB sediment cores are available (Çağatay et al., this issue). Three of these six calibrated  $\text{C}14$  ages are transferred to the AR record. The three lowermost ages could not be transferred unambiguously to the AR record because event deposits are intercalated with banded sediments, which are difficult to correlate between cores. The three uppermost ages were used for

dating the AR record. Five calibrated  $^{14}\text{C}$  ages were used to date the NB record as the lithological unit II provides no other age constraints (Fig. 2). The lowermost available  $^{14}\text{C}$  age (for NB) are in the interval where we tune our record to the NGRIP  $\delta^{18}\text{O}$  record. Although it agrees well with the tuned ages, we do not use these dates in the age model for consistency.

## 2.9. Magnetostratigraphy

The uppermost 110 m of the event-corrected composite record of the AR core has yielded normalized NRM intensity records, by using anhysteretic remanence (ARM), after 20 and 30 mT (mT) of AF peak field demagnetization, to normalize the NRM intensity for changes in concentration of remanence carrying grains downcore. To a first approximation, the normalized NRM record represents an estimate of the relative paleointensity (RPI) of the Earth's magnetic field (Vigliotti et al., this issue). A case can be made that the RPI record is a global signal at millennial (but probably not at centennial) timescales, and therefore provides a valuable means of correlation using the calibrated RPI template known as PISO-1500 (Channell et al., 2009). RPI minima were identified in the AR record and a comparison with PISO-1500 reference template (Table 1). Some of the RPI minima in the AR

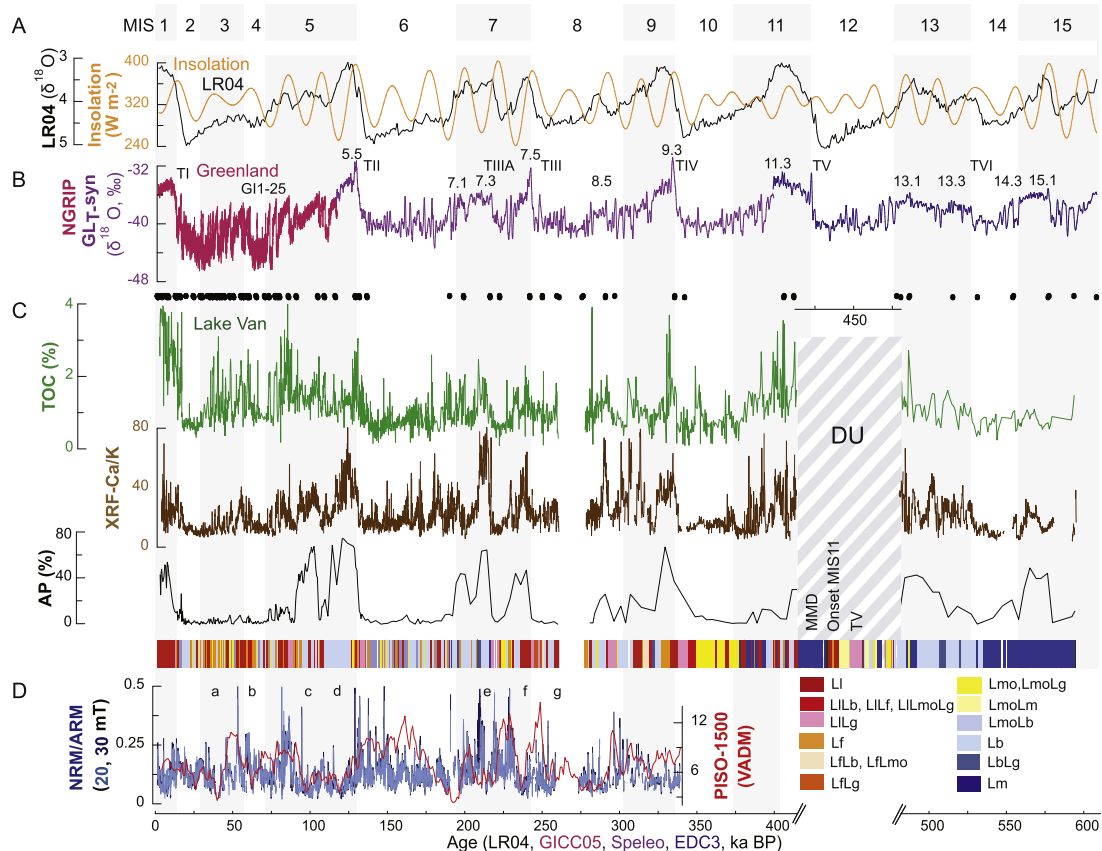


**Fig. 4.** Marine- and ice-core and synthetic isotope chronologies aligned to the Lake Van paleo-climate records. A. LR04 isotopic record (in ‰ VPDB) and the difference between June and December insolation at 39° N, which reflects changes in seasonality (Laskar et al., 2004) documenting the Glacial/Interglacial cycles. B. Ice-core records (NGRIP/GLT-syn, in ‰ VSMOW). C. Lake Van proxy time series of TOC, AP and XRF-Ca/K and the lithology. The DU (Deformed Unit) with the mass-movement deposit (MMD) on top reflects in-situ replaced sediments, which are stratigraphically disturbed but its lithological signature allows identification of the sediments at the onset of MIS11 and the TV (details see Stockhecke et al., 2014). D. Natural remanent magnetization (NRM) normalized by anhysteretic remanence (ARM) after 20 and 30 mT (mT) of AF represents an estimation of the relative paleointensity (RPI) of the earth's magnetic field. Identified minima (a–g) are in agreement with the reference record of the PISO-1500 stack (Channell et al., 2009). The minima at ~41 ka correspond to the Laschamp excursion. Diamonds indicate the age control points given in Table 3. LI: laminated, Lf: faint laminated, Lmo: mottled, Lb: banded, Lm: massive, Lg: graded beds, the combinations reflect intercalations of two or more different lithotypes.

record (label a in Fig. 4) correspond to the geomagnetic excursions within the Brunhes chron (Laj and Channell, 2007). Apart from the apparent identification of the Laschamp (Table 1; Vigliotti et al., this issue), the directional excursions associated with the RPI minima are not identified at Lake Van. Directional excursions are known to be brief (often <1 ka) events that are short relative to the RPI minima in which they are found. For this reason, the directional excursions are often not recorded in sedimentary sections in which the RPI fluctuations are well defined. This is apparently the case in the sediments of Lake Van where the fidelity and resolution of the paleomagnetic directional record is insufficient to record the excursions, but sufficient to yield acceptable RPI records.

### 2.10. $^{10}\text{Be}$ during the Laschamp

About 60  $^{10}\text{Be}$  samples were measured with AMS at the Laboratory of Ion Beam Physics, ETH Zürich (Lachner et al., in preparation) and reveal a Beryllium-10 flux peak in a depth range from 19.8 to 20.7 m cblf (Table 1). This interval is mostly included in the depth (20.06–21.6 m cblf) where the Laschamp event was identified as a low in the RPI record. Moreover the  $^{10}\text{Be}$  peaks are coincident with the paleomagnetic directions indicating an almost full directional change for the magnetic field. The  $^{10}\text{Be}$  signal shows the expected increase in the flux of this radioisotope to the sediment by about a factor of two. Thus both, width and dynamics of the  $^{10}\text{Be}$  signal support the proposed alignment to the NGRIP record.

### 2.11. Linear sedimentation and mass accumulation rates

Wet-bulk densities of the whole rounds were determined by using a Multi Sensor Core Logger (MSCL) in the field. The wet-bulk densities were used to calculate mass accumulation rates (MAR in  $\text{g cm}^{-2} \text{a}^{-1}$ ) according to Niessen et al. (1992). Average TOC contents of 1.15% were used to derive the dry-bulk density ( $-0.047 \times \text{TOC} + 2.6$ ) and porosity (Niessen et al., 1992).

## 3. Results

### 3.1. Chronology of the Northern Basin

The transferred tie points from the AR record and the additional  $^{14}\text{C}$  ages are shown against the event-corrected composite (mcblf-nE) and composite depth (mcblf) in Fig. 2. The age control points are given in Table 2. The constructed age model is comprised of a total of 59 tie points: two marking the top and bottom of the record, five calibrated  $^{14}\text{C}$  ages, 52 ages transposed from the AR chronology (six using varve correlation and 36 using volcanoclastic layers). The sequences covering MIS 1 and 3 are well-constrained. MIS 2 is dated by  $^{14}\text{C}$  ages, but the similarity between the banded sediment and the frequently intercalating event deposits limited the establishment of an event corrected depth scale and consequently led to overestimations of sedimentation rates (non-linearity; Stockhecke et al., 2014). The chronology of MIS 4 and 5 based on stratigraphic correlation is less robust. The linear depth/age relationship supports the constructed chronology.

### 3.2. Chronology of the Ahlat Ridge

The compiled ages from the different methods are shown against the event-corrected composite (mcblf-nE) and composite depth (mcblf) in Fig. 3. The age control points are given in Table 3. Ages are given in thousands of years before present (ka BP), where 0 BP is defined as 1950 AD. Marine isotope stage (MIS) boundaries follow Lisiecki and Raymo (2005) and the nomenclature of the

substages follows Jouzel et al. (2007). Generally, the ages agree and reveal a linear sediment accumulation with time. The climatostatigraphic alignment between the proxy records and ice-core stratigraphy provided the best coverage on age control. The age model was constructed using the 49 tuning-based age control points, the four ages from varve chronology and three calibrated  $^{14}\text{C}$  ages (total 56, red line, Fig. 3A).

The age model of the 1<sup>st</sup> climate cycle (Fig. 1A) is based on tuning, varve chronology and  $^{14}\text{C}$  ages. It is very well constrained and broadly supported by three  $^{40}\text{Ar}/^{39}\text{Ar}$  ages (differences are between 0.4 and 1.4 kyr) and identified RPI minima, including the Laschamp excursion (Fig. 4D). The latter include an interval with reverse polarity constrained by the age model from 38.8 to 43.0 ka BP (Table 1, Vigliotti et al., this issue), within <1 ka of the generally accepted age for this magnetic excursion (41.3 ± 0.6 ka BP, Laj et al., 2014; 40.70 ± 0.95 ka BP; Singer et al., 2009). With the presented age model the  $^{10}\text{Be}$  during this excursion shows

**Table 2**  
Age model for ICDP PALEOVAN drill cores of the NB drill site (5034-1).

Depth (m cblf)	Depth (m cblf-nE)	Age (ka BP)	Error	Event
0.00	0.00	-0.06		2010
1.12	0.39	0.61	0.048	14C
1.36	0.45	0.70		V-1
7.83	1.15	2.35		V-2
13.81	1.53	4.33	0.078	14C
17.11	2.28	6.01		V-4
17.57	2.42	6.89		V-5
17.65	2.49	7.25		V-6
18.66	3.38	11.77		V-7
18.90	3.42	11.69		Onset Holocene
19.08	3.60	11.91		Red ML <sup>a</sup>
20.66	5.05	12.96		V-8
20.78	5.11	13.18		Onset YD
20.79	5.12	13.25		V-10
20.93	5.17	13.46		V-11
20.96	5.18	13.49		V-12
20.96	5.19	13.51		V-13
21.04	5.26	13.53		V-14
21.13	5.33	13.58		V-15
21.35	5.48	14.07		V-16
21.62	5.60	14.64		Onset GI1/B/A
31.12	11.71	18.59	0.062	14C
34.31	14.90	19.72	0.418	14C
34.68	15.28	20.60	0.554	14C
56.69	27.81	28.85		Onset GI4
63.25	32.84	32.45		V-18
76.89	35.52	34.59		V-22
78.00	36.25	35.72		V-23
78.07	36.27	35.77		V-24
78.46	36.66	36.49		V-25
78.72	36.90	37.12		V-26
88.01	43.03	42.91		V-32
89.30	43.59	44.20		V-33
89.44	43.72	44.67		V-34
89.98	44.09	46.02		V-35
91.64	44.70	48.81		V-36
94.60	47.04	53.48		V-37
96.45	47.78	56.80		V-39
96.55	47.86	57.14		V-40
96.71	47.96	57.58		V-41
97.03	48.09	58.06		V-42
97.19	48.21	58.38		V-43
97.33	48.24	58.54		Onset GI17
104.27	51.95	62.03		V-51?
106.31	52.49	63.19		V-52?
106.78	52.70	64.36		V-53?
120.26	61.24	70.61		V-57?
135.63	69.40	81.35		V-60?
145.40	76.73	90.53		Extrapolation 0.76 mm/a <sup>b</sup>

<sup>a</sup> Landmann et al., 1996 10.59 ka BP.

<sup>b</sup> Avg LSR, 0.76 mm/yr.

**Table 3**

Age model for ICDP PALEOVAN drill cores of the AR drill site (5034-2). Errors refer to the dating error of the original reference timescale and do not include the additional error related to climatostratigraphic alignment (n.s.: not specified).

Depth (mcbf)	Depth (mcbf-nE)	Age (ka BP)	Error	Event	Timescale	References
0.0000	0.0000	-0.060		2010		
0.3570	0.3570	0.610	0.048	14C		
1.5831	1.5297	2.672	0.025	V-3a	Varvecount	Landmann et al., 1996
2.2881	2.1504	4.330	0.078	14C		
2.9030	2.7598	6.005	0.06	V-4	Varvecount	Landmann et al., 1996
3.2551	3.1081	6.888	0.069	V-5	Varvecount	Landmann et al., 1996
3.3451	3.1921	7.192	0.072	V-6	Varvecount	Landmann et al., 1996
4.6055	4.4432	11.653	0.099	Onset Holocene, YDPB	NGRIP GICC05	Blockley et al., 2012
5.9449	5.6235	12.846	0.138	Onset YD	NGRIP GICC05	Blockley et al., 2012
6.5912	6.1959	14.642	0.186	Onset GI1/B/A	NGRIP GICC05	Blockley et al., 2012
8.9026	8.5026	18.590	0.062	14C		
11.0467	10.6467	23.290	0.596	Onset GI2	NGRIP GICC05	Blockley et al., 2012
13.4224	13.0141	27.730	0.832	Onset GI3	NGRIP GICC05	Blockley et al., 2012
14.0495	13.6358	28.850	0.898	Onset GI4	NGRIP GICC05	Blockley et al., 2012
14.7298	14.2501	32.450	1.132	Onset GI5	NGRIP GICC05	Blockley et al., 2012
18.2773	14.5738	33.690	1.212	Onset GI6	NGRIP GICC05	Blockley et al., 2012
18.8590	15.1375	35.430	1.321	Onset GI7	NGRIP GICC05	Blockley et al., 2012
19.8290	16.0496	38.170	1.449	Onset GI8	NGRIP GICC05	Blockley et al., 2012
20.6297	16.7982	40.110	1.58	Onset GI9	NGRIP GICC05	Blockley et al., 2012
21.0384	17.2069	41.410	1.633	Onset GI10	NGRIP GICC05	Blockley et al., 2012
21.6747	17.7166	43.290	0.868	Onset GI11	NGRIP GICC05	Svensson et al., 2008
22.6758	18.6763	46.810	0.956	Onset GI12	NGRIP GICC05	Svensson et al., 2008
23.4575	19.4180	49.230	1.015	Onset GI13	NGRIP GICC05	Svensson et al., 2008
24.7558	20.7084	54.170	1.15	Onset GI14	NGRIP GICC05	Svensson et al., 2008
25.2198	21.1601	55.750	1.196	Onset GI15	NGRIP GICC05	Svensson et al., 2008
26.1939	22.0811	58.230	1.256	Onset GI16	NGRIP GICC05	Svensson et al., 2008
26.5792	22.4134	59.000	1.287	Onset GI17 <sup>a</sup>	NGRIP GICC05	Svensson et al., 2008
29.9860	24.3682	64.045	n.s.	Onset GI18	NGRIP GICC05	Wolff et al., 2010
31.8241	26.0922	69.580	n.s.	Onset GI18.1	NGRIP GICC05	Wolff et al., 2010
33.3264	27.1486	72.280	n.s.	Onset GI19	NGRIP GICC05	Wolff et al., 2010
34.8068	28.4493	76.400	n.s.	Onset GI20	NGRIP GICC05	Wolff et al., 2010
35.4748	29.0750	77.980	n.s.	Peak GI20.1	NGRIP GICC05	
36.0202	29.5317	79.170	n.s.	Peak GI20.2	NGRIP GICC05	
40.4590	31.7614	84.970	n.s.	Onset GI21	NGRIP GICC05	
44.6025	34.9739	90.030	n.s.	Onset GI22	NGRIP GICC05	Chapron et al., 2010
48.5420	38.7100	104.030	n.s.	Onset GI23	NGRIP GICC05	Chapron et al., 2010
50.6820	40.3994	108.270	n.s.	Onset GI24	NGRIP GICC05	Chapron et al., 2010
53.1058	42.5715	115.400	n.s.	Onset GI25	NGRIP GICC05	
56.9052	45.9886	128.400	1.25	Peak MIS5.5	GLT_syn SpeleoAge	Barker et al., 2011
57.8703	46.8463	131.000	1.25	Onset MIS5.5 <sup>b</sup>	GLT_syn SpeleoAge	Barker et al., 2011
61.2747	49.1515	136.000	1.25	Onset TII	GLT_syn SpeleoAge	Barker et al., 2011
95.6002	74.9107	189.500	2.6	Onset 6×	GLT_syn SpeleoAge	Barker et al., 2011
99.3030	78.0752	198.800	2.2	Peak MIS7.1	GLT_syn SpeleoAge	Barker et al., 2011
104.0491	82.6583	216.000	2.15	Peak MIS7.3	GLT_syn SpeleoAge	Barker et al., 2011
107.6259	85.1541	222.200	1.35	Onset TIIIA	GLT_syn SpeleoAge	Barker et al., 2011
113.2171	90.2816	241.800	0.25	Peak MIS7.5	GLT_syn SpeleoAge	Barker et al., 2011
118.1360	93.5414	250.000	0.25	Onset TIII	GLT_syn SpeleoAge	Barker et al., 2011
121.5290	96.3986	259.461	1.55	Extrapolation <sup>c</sup>	GLT_syn SpeleoAge	Barker et al., 2011
<b>Gap – No interpolation</b>						
130.0720	96.3987	276.863	1.45	Extrapolation <sup>c</sup>	GLT_syn SpeleoAge	Barker et al., 2011
135.2130	100.6680	291.000	1.4	Onset MIS8.5	GLT_syn SpeleoAge	Barker et al., 2011
136.1480	101.3376	297.000	1	Minima before MIS8.5	GLT_syn SpeleoAge	Barker et al., 2011
144.8905	107.5665	336.000	2.47	Onset MIS9.3 <sup>b</sup>	GLT_syn SpeleoAge	Barker et al., 2011
147.8000	109.7001	351.000	0.83	Onset TIV	GLT_syn SpeleoAge	Barker et al., 2011
158.0000	118.5391	392.000	n.s.	Peak MIS11.1	GLT_syn SpeleoAge	Barker et al., 2011
160.7960	121.2282	407.000	n.s.	Peak MIS11.3	GLT_syn GDC3Age	Barker et al., 2011
163.6940	123.1266	413.285	n.s.	Extrapolation <sup>c</sup>	GLT_syn GDC3Age	Barker et al., 2011
<b>Gap – No Interpolation</b>						
186.1050	144.6207	480.067	n.s.	Extrapolation <sup>d</sup>	GLT_syn GDC3Age	Barker et al., 2011
187.8170	146.1734	488.500	n.s.	Peak MIS13.1	GLT_syn GDC3Age	Barker et al., 2011
195.0000	151.6882	528.000	n.s.	Onset MIS13.3	GLT_syn GDC3Age	Barker et al., 2011
200.5660	156.7461	556.000	n.s.	MIS14.3	GLT_syn GDC3Age	Barker et al., 2011
206.7010	162.7903	579.000	n.s.	MIS15.1	GLT_syn GDC3Age	Barker et al., 2011
210.7590	165.6867	595.213	n.s.	Extrapolation <sup>d</sup>		

Errors refer to the dating error of the original reference and do not include the additional error related to climatostratigraphic alignment (n.s.: not specified).

<sup>a</sup> Differ from table as this tie point is more confidential.

<sup>b</sup> Mid-point.

<sup>c</sup> Avg LSR, 0–158mcbf-nE, 0.3 mm/yr.

<sup>d</sup> Avg LSR, 187–206mcbf-nE, 0.18 mm/yr.

maximum fluxes for a time range between 38.1 and 40.3 ka (Table 1). An error of about 1.6 ka is given for the onset of DO 10 of the GICC05 age model (Table 2, Blockley et al., 2012). The tuned age model and independent dating are thus in good agreement. Sediment accumulation changes are documented by MAR variations from 0.01 to 0.03 g cm<sup>-2</sup> a<sup>-1</sup> (Fig. 3C) over the last 130 kyr. The Holocene, MIS 3 and MIS 5 have similar MARs, while MIS 2 has MARs twofold higher rates. During the full development of MIS 5, the MAR increases slightly. Both trends, the higher MARs of MIS 2 and MIS 4 are in line with the expectation of increased total mass accumulation during cold conditions because of increased eolian input and erosion from open vegetation within the catchment.

The tuned age model of the 2<sup>nd</sup> last climate cycle is supported by two RPI minima (associated with known magnetic excursions) and by four <sup>40</sup>Ar/<sup>39</sup>Ar ages. Alignment to the absolutely-dated reference templates and <sup>40</sup>Ar/<sup>39</sup>Ar dating resulted in an acceptable consistency between 6 and 17 ka. The MARs are slightly higher during the 2<sup>nd</sup> climate cycle as compared to the 1<sup>st</sup> one, although lithologies are generally similar.

The age model of the 3<sup>rd</sup> climate cycle is confirmed by a very good match with one <sup>40</sup>Ar/<sup>39</sup>Ar age, and one identified minima in the RPI record. The linear sedimentation rates (LSR) of MIS8 are partly extrapolated (red dashed lines Fig. 3A) on account of a supposed gap, which is estimated to last ~17 kyr (260–277 ka BP) and is related to the deposition of ~10 m-thick volcaniclastic material (V-206), which probably eroded some of the background sediment. Obviously, LSRs and MARs within the extrapolated cannot be adequately estimated. Nevertheless, the depth–age relationship of the 3<sup>rd</sup> glacial cycle inflects that of the 2<sup>nd</sup> one and, accordingly, LSR decrease from 0.3 to 0.1 mm a<sup>-1</sup>. One explanation is that each of the event layers in this interval, eroded the underlying sediments.

A good match between the lithology, TOC, Ca/K and AP pollen and the GL<sub>T</sub>-syn record allow to assign the sediments from the upper boundary of the Deformed Unit (DU) to MIS11, i.e., to the 4<sup>th</sup> climate cycle, although the onset of MIS11 is stratigraphically disturbed (see detail in Stockhecke et al., 2014). The upper and lower boundary of the DU are dated (by extrapolation of sedimentation rates), but ages between 413 and 480 ka can not be interpolated (Table 3) as this interval lacks independent age constraints. However, lithological changes are characterized by generally lower MARs compared to those of the 1<sup>st</sup> and 2<sup>nd</sup> climate cycle.

The robustness of the age for the undisturbed part of the 5<sup>th</sup> and 6<sup>th</sup> climate cycle is confirmed by one <sup>40</sup>Ar/<sup>39</sup>Ar age. Note that the different sedimentological regime and the low resolution of the proxy data increase the likelihood of an erroneous match between the proxy records and the synthetic ice-core chronology. However, the observed change in MARs is anticipated: It reflects the change from freshwater conditions with depositions of diatomaceous mud to the present-day soda and alkaline water conditions with depositions of carbonaceous clayey silt (Stockhecke et al., 2014).

#### 4. Conclusion

The compilation of the ages derived by different methods confirms that the record covers six Glacial/Interglacial cycles. The alignment of the proxy records to the Greenland stadials/interstadial on the GICC05 timescale results in a millennial-scale resolved synchronization. The presented chronology is based on GICC05/GICC05modeltext from 0 to 116 ka BP, the absolutely-dated and precise timescale of the Chinese speleothem records from 116 to 400 ka, and the EDC timescale from Antarctica ice cores for 400 to 600 ka. Seven geomagnetic tie points (from 39 to 259 ka), based on minima in the RPI record, and nine <sup>40</sup>Ar/<sup>39</sup>Ar ages confirm the age model. However, uncertainties increase with depth as tectonic

activity affected the drill site and the sedimentary regime was completely different during the early evolution of Lake Van. Excluding two major gaps, the 166-m-long event corrected AR record reflects continuous sedimentation over the last ~600 kyr.

The NB record contains several unconformities in the lowermost part, and the thicker and more frequent event deposits. Thus, the age model is less well constrained than the AR site and the record covers ~90 kyr. Geochemical fingerprinting of the volcaniclastic layers will allow the chronology to be improved by tephrostratigraphy. We conclude that the AR age model enables the investigation of annual- to centennial climate variability of the Holocene, centennial- to millennial scale of the Last Glacial/Interglacial cycle, and multi-millennial variability for the 2<sup>nd</sup> to 6<sup>th</sup> last climate cycles. The NB age model serves to date event deposits precisely and to establish an event catalog within a context of millennial scale climate change. The widely supported chronology of the AR record, based on a variety of independent methods, facilitates reconstructions and modeling of Quaternary climate evolution in the Near East over the past ~600 kyr. Moreover, the chronostratigraphy for the last 250 kyr provides a useful reference to test and improve other dating methods.

#### Acknowledgments

We thank the PaleoVan team for support during collection and sharing of data. In particular, we thank Hans-Ulrich Schmincke and Mari Sumita for providing the <sup>40</sup>Ar/<sup>39</sup>Ar ages. The authors acknowledge funding of the PaleoVan drilling campaign by the International Continental Scientific Drilling Program (ICDP), the Deutsche Forschungsgemeinschaft (DFG), the Swiss National Science Foundation (SNF) 200021\_124981 and 200020\_143330 and the Scientific and Technological Research Council of Turkey (Tübitak). Thanks go to A. Feray Göktepe, Sefer Örcen and Mustafa Karabiyikoglu from the Yüzüncü Yıl Üniversitesi of Van, Turkey, for their cooperation and support, and to the ship's crew, Mete Orhan, Mehmet Sahin, and Münip Kanan for their strong commitment. Thanks also go to Ulla Röhl, Alex Wuijers, Hans-Joachim Wallrabe-Adams, Vera Lukies and Holger Kuhlmann from the IODP Core Repository Bremen for their help during the sampling parties. The manuscript benefited from the constructive comments of two anonymous reviewers and excellent editorial handling.

#### References

- Austin, W.E.N., Hibbert, F.D., 2010. Tracing time in the ocean: a brief review of chronological constraints (60–8 kyr) on North Atlantic marine event-based stratigraphies. *J. Quat. Sci.* 36, 28–37.
- Bar-Matthews, M., Ayalon, A., Kaufman, A., Wasserburg, G.J., 1999. The Eastern Mediterranean paleoclimate as a reflection of regional events: Soreq Cave, Israel. *Earth Planet. Sci. Lett.* 166, 85–95.
- Barker, S., Knorr, G., Edwards, L., Parrenin, F., Putnam, A.E., Skinner, L.C., Wolff, E., Ziegler, M., 2011. 800,000 Years of abrupt climate variability. *Science* 334, 347–351.
- Blockley, S.P.E., Lane, C.S., Hardima, M., Rasmussen, S.O., Seierstad, I.K., Steffensen, J.P., Svensson, A., Lotter, A.F., Turney, C.S.M., Ramsey, C.B., INTIMATE members, 2012. Synchronisation of palaeoenvironmental records over the last 60,000 years, and an extended INTIMATE<sup>1</sup> event stratigraphy to 48,000 b2k. *Quat. Sci. Rev.* 36, 2–10.
- Broecker, W.S., Bond, G., Klas, M., Bonani, G., Wolfli, W., 1990. A salt oscillator in the glacial Atlantic? I. The concept. *Paleoceanography* 5 (4), 469–477.
- Çağatay, N., Ogretmen, N., Damci, E., Stockhecke, M., Sancar, Ü., Eris, K.K., Ozeren, S., 2014. Paleoclimate and Lake Level Records From the Northern Basin of Lake Van, Turkey (this issue).
- Cheng, H., Edwards, R.L., Broecker, W.S., Denton, G.H., Kong, X., Wng, Y., Zhang, R., Wanf, Xianfeng, 2009. Ice Age terminations. *Science* 326 (5950), 248–252.
- Channell, J.E.T., Xuan, C., Hodell, D.A., 2009. Stacking paleointensity and oxygen isotope data for the last 1.5 Myrs (PISO 1500). *Earth Planet. Sci. Lett.* 283, 14–23.
- Chapron, E., Landais, A., Chappellaz, J., Schilt, A., Buiron, D., Dahl-Jensen, D., Johnsen, S.J., Jouzel, J., Lemieux-Dudon, B., Loulergue, L., Leuenberger, M., Masson-Delmotte, V., Meyer, H., Oerter, H., Stenni, B., 2010. Millennial and sub-

- millennial scale climatic variations recorded in polar ice cores over the Last Glacial period. *Clim. Past* 6, 345–365.
- Deplazes, G., Luckge, A., Peterson, L.C., Timmermann, A., Hamann, Y., Hughen, K.A., Röhl, U., Laj, C., Cane, M.A., Sigman, D.M., Haug, G.H., 2013. Links between tropical rainfall and North Atlantic climate during the Last Glacial period. *Nat. Geosci.* 6 (3), 213–217.
- Fleitmann, Cheng, H., Badertscher, S., Edwards, R.L., Mudelsee, M., Göktürk, O.M., Fankhauser, A., Pickering, R., Raible, C.C., Matter, A., Kramers, J., Tüysüz, O., 2009. Timing and climatic impact of Greenland interstadials recorded in stalagmites from northern Turkey. *Geophys. Res. Lett.* 36, L19707 <http://dx.doi.org/10.1029/2009GL040050>.
- Jouzel, J., Masson-Delmotte, V., Cattani, O., Dreyfus, G., Falourd, S., Hoffmann, G., Minster, B., Jouet, J., Barnola, J.M., Chappellaz, J., Fischer, H., Gallet, J.C., Johnsen, S., Leuenberger, M., Louergue, L., Luethi, D., Oerter, H., Parrenin, F., Raisbeck, G., Raynaud, D., Schilt, A., Schwander, J., Selmo, E., Souchez, R., Spahni, R., Stauffer, B., Steffensen, J.P., Stenni, B., Stocker, T.F., Tison, J.L., Werner, M., Wolff, E.W., 2007. Climate variability over the past 800 000 years. *Science* 317, 793.
- Kwicien, O., Stockhecke, M., Pickarski, N., Heumann, G., Litt, T., Sturm, M., Anselmetti, F.S., Haug, G.H., 2014. Dynamics of the Last Four Glacial Terminations Recorded in Lake Van, Turkey (this issue).
- Lachner, J., Stockhecke, M., Beer, J., 2014. Highly Resolved  $^{10}\text{Be}$  Record of the Laschamp Event at Lake Van (in prep.).
- Laj, C., Channell, J.E.T., 2007. Geomagnetic excursions. In: Kono, M. (Ed.), *Treatise on Geophysics. Geomagnetism*, vol. 5. Elsevier, Amsterdam, pp. 373–416.
- Laj, C., Guillou, H., Kissel, C., 2014. Dynamics of the earth magnetic field in the 10–75 kyr period comprising the Laschamp and Mono Lake excursions: new results from the French Chaîne Puys in a global perspective. *Earth Planet. Lett.* 387, 184–197.
- Landmann, G., Reimer, A., Lemcke, G., Kempe, S., 1996. Dating Late Glacial abrupt climate changes in the 14,570 yr long continuous varve record of Lake Van, Turkey. *Palaeogeogr. Palaeoclimatol. Palaeoecol.* 122, 107–118.
- Laskar, J., Robutel, P., Joutel, F., Gastineau, M., Correia, A., Levrard, B., 2004. A long-term numerical solution for the insolation quantities of the earth. *Astron. Astrophys.* 428, 261–285.
- Lemcke, G., 1996. Paläoklimarekonstruktion am Van See (Ostanatolien, Türkei) (Ph.D. thesis). Swiss Federal Institute of Technology, Zurich. ETH no.11786, 182 p.
- Lemcke, G., Sturm, M., 1997.  $\delta^{18}\text{O}$  and trace element measurements as proxy for the reconstruction of climate changes at Lake Van (Turkey): preliminary results. *NATO ASI Ser.* 149, 653–678.
- Lisiecki, L.E., Raymo, M.E., 2005. A Pliocene-Pleistocene stack of 57 Globally Distributed Benthic  $\delta_{18}\text{O}$  Records, Paleceanography, 20, PA1003, Data archived at the World Data Center for Paleoclimatology. Boulder, Colorado, USA.
- Litt, T., Krastel, S., Sturm, M., Kipfer, R., Örcen, S., Heumann, G., Franz, S.O., Ülgen, U.B., Niessen, F., 2009. 'PALEOVAN', International Continental Scientific Drilling Program (ICDP): site survey results and perspectives. *Quat. Sci. Rev.* 28, 1555–1567.
- Litt, T., Anselmetti, F.S., Baumgarten, H., Beer, J., Çağatay, N., Cukur, D., Damci, E., Glombitza, C., Heumann, G., Kallmeyer, J., Kipfer, R., Krastel, S., Kwicien, O., Meydan, A.F., Örcen, S., Pickarski, N., Randlett, M.-E., Schmincke, H.-U., Schubert, C.J., Sturm, M., Sumita, M., Stockhecke, M., Tomonaga, Y., Vigliotti, L., Wonik, T., the PALEOVAN Scientific Team, 2012. 500,000 Years of environmental history in eastern Anatolia: the PALEOVAN drilling project. *Sci. Drill.* 14, 18–29 <http://dx.doi.org/10.2204/iodp.sd.14.02.2012>.
- Litt, T., Pickarski, N., Heumann, G., Stockhecke, M., Tzedakis, C., 2014. A 600,000 Year Long Continental Pollen Record from Lake Van, Eastern Anatolia (Turkey) (this issue). <http://dx.doi.org/10.1016/j.quascirev.2014.03.017>.
- Melles, M., Brigham-Grette, J., Minyuk, P.S., Nowaczyk, N.R., Wennrich, V., DeConto, R.M., Anderson, P.M., Andreev, A.A., Coletti, A., Cook, T.L., Haltia-Hovi, E., Kukkonen, M., Lozhkin, A.V., Rosen, P., Tarasov, P., Vogel, H., Wagner, B., 2012. 2.8 million years of arctic climate change from Lake El'Gygtygyn, ne Russia. *Science* 337, 315–320.
- North Greenland Ice Core Project members (NGRIP), 2004. High-resolution record of Northern Hemisphere climate extending into the Last Interglacial period. *Nature* 431, 147–151.
- Niessen, F., Wick, L., Bonani, G., Chondrogianni, C., Siegenthaler, C., 1992. Aquatic system response to climate and human changes: productivity, bottom water oxygen status, and sapropel formation in Lake Lugano over the last 10 000 years. *Aquat. Sci.* 54, 257–276.
- Singer, B.S., Guillou, H., Jicha, B.R., Laj, C., Kissel, C., Beard, B.L., Johnson, C.M., 2009.  $^{40}\text{Ar}/^{39}\text{Ar}$ , K/Ar and  $^{230}\text{Th}/^{238}\text{U}$  dating of the Laschamp excursion: a radioisotopic tie-point for ice core and climate chronologies. *Earth Planet. Sci. Lett.* 286, 80–88.
- Steffensen, J.P., Andersen, K.K., Bigler, M., Clausen, H.B., Dahl-Jensen, D., Fischer, H., Goto-Azuma, K., Hansson, M., Johnsen, S.J., Jouzel, J., Masson-Delmotte, V., Popp, T., Rasmussen, S.O., Röhlisberger, R., Ruth, U., Stauffer, B., Siggaard-Andersen, M.L., Sveinbjörnsdóttir, A.E., Svensson, A., White, J.W.C., 2008. High-resolution Greenland Ice Core data show abrupt climate change happens in few years. *Science* 321 (5889), 680–684.
- Svensson, A., Anderson, K.K., Bigler, M., Clausen, H.B., Dahl-Jensen, D., Davies, S.M., Johnsen, S.J., Muscheler, R., Parrenin, F., Rasmussen, S.O., Röhlisberger, R., Seierstad, I., Steffensen, J.P., Vinther, B.M., 2008. A 60,000 year Greenland stratigraphic ice core chronology. *Clim. Past* 4, 47–57.
- Stockhecke, M., Sturm, M., Brunner, I., Schmincke, H.-U., Sumita, M., Kwicien, O., Cukur, D., Anselmetti, F.S., 2014. Sedimentary evolution and history of Lake Van (Turkey) over the past 600,000 years. *Sedimentology* (in press). <http://dx.doi.org/10.1111/sed.12118>.
- Sumita, M., Schmincke, H.-U., 2013a. Impact of volcanism on the evolution of Lake Van II: temporal evolution of explosive volcanism of Nemrut Volcano (eastern Anatolia) during the past ca. 0.4 Ma. *J. Volcanol. Geotherm. Res.* 253, 15–34 <http://dx.doi.org/10.1016/j.jvolgeores.2012.12.009>.
- Sumita, M., Schmincke, H.-U., 2013b. Erratum to "Impact of volcanism on the evolution of Lake Van II: temporal evolution of explosive volcanism of Nemrut Volcano (eastern Anatolia) during the past ca. 0.4 Ma." *J. Volcanol. Geotherm. Res.* 253, 131–133 <http://dx.doi.org/10.1016/j.jvolgeores.2013.01.008>.
- Sumita, M., Schmincke, H.-U., 2013c. Impact of volcanism on the evolution of Lake Van I: evolution of explosive volcanism of Nemrut Volcano (eastern Anatolia) during the past ca. 0.4 Ma. *Bull. Volcanol.* 75, 714.
- Vigliotti, L., Channell, J.E.T., Stockhecke, M., 2014. Paleomagnetism of Lake Van sediments: chronology and paleoenvironment since 350 ka. (this issue).
- Wang, Y.J., Cheng, H., Edwards, R.L., An, Z.S., Wu, J.Y., Sheen, C.C., Doral, J.A., 2001. A high-resolution absolute-dated Late Pleistocene monsoon record from Hulu Cave, China. *Science* 294, 2345–2348.
- Wang, Y., Cheng, H., Edwards, R.L., Xinggong Kong, X., Shao, X., Chen, S., Wu, J., Jiang, X., Wang, X., An, Z., 2008. Millennial- and orbital-scale changes in the East Asian monsoon over the past 224,000 years. *Nature* 451, 1090–1093.
- Wolff, E.W., Chappellaz, J., Blunier, T., Rasmussen, S.O., Svensson, A., 2010. Millennial-scale variability during the Last Glacial: the ice core record. *Quat. Sci. Rev.* 29 (21–22), 2828–2838.